Differential basal-to-apical accessibility of lamin A/C epitopes in the nuclear lamina regulated by changes in cytoskeletal tension

Teemu O. Ihalainen[1,2†], Lina Aires[1†], Florian A. Herzog[1], Ruth Schwartlander[1], Jens Moeller[1] and Viola Vogel*[1]

[1] Laboratory of Applied Mechanobiology, Department of Health Sciences and Technology, ETH Zurich, Switzerland
[2] NeuroGroup, BioMediTech, University of Tampere, Tampere, Finland

[†] these authors contributed equally

Supplemental Materials and Methods

DNA constructs

N-terminally EGFP tagged human wild-type (wt) lamin A (EGFP-lam A) was originally obtained by wt-lamin A cDNA insertion into the EGFP-C1 plasmid (Clontech) and expression under the CMV promoter (generous gift from Dr. Maija Vihinen-Ranta). This construct was further used to produce a second lamin A construct without fused EGFP (lam A) and additional lamin A EGFP fused mutants: EGFP-ΔN20-Lamin A, P-null, R482Q and K486N. The EGFP-ΔN20-Lamin A mutant lacks the first 20 amino acids of the lamin A, P-null is a phosphorylation negative mutant within the LA/C-C epitope sequence (ε_{c1}) obtained by 4 point mutations (S390A, S392A, S395A and S404A). R482Q, as well as, K486N correspond to single point mutations within lamin A for the respective residues. The mutants were constructed and sequenced by GenScript. EGFP-KASH2 and EGFP-KASH2ext were kindly provided by Dr. Didier Hodzic (Washington University School of Medicine, St. Louis).

Immunolabeling

The cells (NIH 3T3 fibroblasts, MEFs or hMSC) were first incubated with permeabilization buffer (0.1 % Triton-X 100, 0.5 % BSA and 0.1 % Na-Azide in PBS) for 10 min at room temperature (RT). Cells were then labeled with the primary antibody for 1 h at RT, followed with 3 washes (permeabilization buffer, then PBS and followed by permeabilization buffer) of 10 min each. Next, the cells were incubated with the secondary antibody with or without phalloidin for 30 min at RT, in the dark. Finally, cells were washed for 2 times with PBS for

10 min each. Samples were embedded in Prolong Gold with or without DAPI (Invitrogen) and stored at RT for 24 h and then at + 4 ºC. The samples were imaged within 2 weeks from the immunolabeling. All the antibodies and phalloidins were diluted in 3 % BSA in PBS. The primary antibodies were diluted 1:200 for LA/C-C (Abcam, ab8984) and LA (Abcam, ab8980), 1:500 for LA/C-N (Santa-Cruz Biochemicals, sc-6215), LB1 (Abcam, ab16048), Nesprin 2 (ImmuQuest, IQ565) and Nesprin 3 (ImmuQuest, IQ566), 1:100 for LC (Abcam, ab106682), HP1 (Abcam, ab77256) and Emerin (Abcam, ab40688), 1:1000 for SUN2 (generous gift from Dr. Ulrike Kutay). Secondary antibodies linked with Alexa-488, -555 or -633 (Invitrogen), were diluted 1:200. Phalloidin Alexa-488 or -633 was used at a dilution of 1:200 and 1:50, respectively. PPARγ antibody (I-18) (Santa Cruz Biochemicals, sc-6285) and alkaline phosphatase (L-19) (Santa Cruz Biochemicals, sc-15065), were used at 1:50 dilution as pre-adipocyte and pre- osteocyte hMSC differentiation markers, respectively.

Cells on Fn-coated glass and on Fn-coated polyacrylamide (PAA) hydrogels

In the cell spreading experiments, 3000 cells / cm^2 were seeded per well of a 6-well-plate having 1 coverslip. For each experiment, cells were allowed to spread for the indicated times and were subsequently fixed with 2 % paraformaldehyde in PBS for 10 min at RT. Cells were stored in PBS at + 4 ºC. Immunolabeling was performed within a week after fixation.

Confocal microscopy and image processing.

Samples were imaged either with a SP5 (Leica) or LSM780 (Zeiss) confocal microscope. Single nuclei and single cell imaging was conducted using a 63x/1.4 oil immersion objective. Larger fields were imaged using a 20x/0.7 dry objective. DAPI was excited with 405 nm, EGFP and Alexa-488 with 488 nm, Alexa-555 with 561 nm and Alexa-633 with 633 nm lasers. The laser intensities were maintained low in order to avoid photobleaching. The emission bands were 415 – 465 nm, 498 – 548 nm, 571 – 621 nm and 643 – 743 nm for DAPI, Alexa-488 or EGFP, Alexa-555 and Alexa-633 respectively. The PMT gains were adjusted between the images to avoid over/under-exposure. When imaging single nuclei, the voxel size was adjusted between 55 – 75 nm in the xy-plane and 150-200 nm in the z-direction. Larger fields were imaged with a pixel size of 200 nm. The image sizes were from 512 x 512 to 2048 x 2048 pixels. The channels were collected sequentially and by using line averaging of 2 or 4.

The image stacks of single cells and nuclei were deconvolved using Huygens Essential software (SVI, Hilversum, Netherlands). A theoretical point spread function was used for the iterative deconvolution process. The refractive index of the embedding medium was determined based

on the available information (Invitrogen) on the time dependence between the refractive index of the Prolong Antifade and the embedding time of the samples. The deconvolution was performed with the following software parameters, the image signal to noise ratio used in the deconvolution was 5, the quality threshold was 0.01 and maximum iterations a total of 200. The deconvolution results were carefully compared to the original data to verify the outcomes.

Subsequent image processing was accomplished using ImageJ[1]. To quantify the nuclei aspect ratios, the nuclei were first segmented from the lamin image stacks. This was accomplished in several phases: first, a maximum intensity projection (MIP) in the xy-plane was made from the stack. Then the average intensity of the whole MIP image was quantified. This average intensity was used 3 times as a threshold to segment the nucleus area in the MIP image. This ratio was found to provide for a good separation of the nucleus from the background. The segmented nucleus area was then used as a mask to measure the mean intensity of the nucleus area in the MIP. Half of this resulting intensity was used to segment the nucleus from the original 3D-stack. Next, MIP of the segmented 3D nucleus was projected in the xy-plane and an ellipse fitting was performed, yielding information about the orientation of the nucleus. This orientation was then used to rotate the segmented nucleus data (whole stack) to yield nuclei with major axis oriented along the y-axis of the images. MIPs were later conducted in xy- and yz-planes. The ellipse fitting was performed to the resulting MIPs to yield aspect ratios in xy- and yz-planes, along with projected nucleus area and circularity. Cell areas and shapes were quantified by first smoothing the undeconvolved data with 5x5 Gaussian kernel and by segmenting the cell boundaries from the images. The segmentation threshold was determined manually. Next, the cell areas, circularity and aspect ratios were measured similarly as described here for the nuclei shapes.

The apical-to-basal lamin intensity ratios were determined by taking a cross section from the middle of the nucleus. The intensities were then measured from a 1.5 – 2 µm wide straight line pointing along the z-direction utilizing the cross section images. The apical-to-basal actin ratios were measured by first determining the geometrical center of the nuclei (the nuclei were segmented as above) and by measuring the highest phalloidin intensity form a 4 * 4 µm area from above and below the nucleus. All figures in the manuscript were compiled using Adobe Photoshop CS6 and Adobe Illustrator CS6 (Adobe Systems, San Jose, US).

PAA-cushion experiments

Uncoated PAA gels used as cushion were fabricated similarly as for the cell cultures. Briefly, the glass coverslips, 8 mm in diameter, were incubated with 3-aminopropyltriethoxysilane

(APTES) at room temperature for 3 min. The coverslips were washed 3x with nanopure water (Millipore) and incubated for 30 min with 0.5% glutaraldehyde (GA) in PBS at pH 7.4. These surfaces were again washed 3x with water and dried in air. Next, a small metallic washer 6.4 mm in diameter (m = 107 mg) was glued on to the bottom of the glass coverslip. The glass coverslips were placed to the bottom of 1.5 ml Eppendorf tube cap (washer side down) and the cap was subsequently filled with the PAA solutions to yield the specified PAA bulk rigidities[2] (0.48 kPa, 1.1 kPa or 4.5 kPa). The filled-in cap was covered with a clean glass coverslip and the gels were allowed to polymerize for 60 min at 37°C.

The cells were cultured on Fn-coated glass coverslips or on 0.48kPa Fn-coated PAA gels, in DMEM (#31966-021, Life-technologies) with 10% serum (FBS, #F9665, Sigma-Aldrich). 24 h after seeding, the cells were subjected to a 5 µg/ml Cytochalasin D treatment for 75 min (for cells seeded on Fn-glass) or 60 min (for cells seeded on Fn-PAA). The medium was then replaced with fresh DMEM (serum free) containing 5µg/ml Cytochalasin D and the cushion PAA hydrogel (diameter 8.4 mm) was carefully placed on top of the cells (Fig. 5d-k, S8). Finally a small metallic washer (diameter 8.8 mm, mass m = 281 mg) was placed on top of the gel, yielding a total pressure of 70 Pa (Fig. S8). After medium exchange, the control cells were kept in serum free DMEM with 5µg/ml Cytochalasin D. Both samples were placed in the cell culture incubator (at 37 °C). After either 45 min for cells seeded on Fn-glass, or 30 min for cells seeded on Fn-PAA), the cells under the PAA-cushion and the control cells were fixed by adding PFA directly to the cell culture medium (final concentration 2 %) followed by a 30 min incubation at RT. After fixation, the gels were carefully removed and the samples were immunolabeled.

Steered molecular dynamics (SMD) simulations

Following well established protocols[3], steered molecular dynamics (SMD) simulations were performed with NAMD[4] using the CHARMM27 force fields[5]. The Ig-like domain of human lamin A/C (pdb: 1IVT,[6]) was immersed in a water box filled with TIP3P molecules[7] with at least 15 Å padding between the protein and the box edge in all directions using the Solvate plugin in VMD[8] and neutralized at 0.15 M salt concentration. For the equilibration, the system was minimized for 2000 steps while keeping protein atoms fixed and further 2000 steps without restrains. The system was then thermalized to 310 K by raising the temperature 3.1 K every 100 steps and equilibrated for 10 ns. For the SMD simulations, the water box was adjusted to either 150 Å or 337 Å in the direction defined by the force vector. Constant tensile forces were then applied on the carbon alpha atoms of S428 and V549 in opposite direction but with equal

magnitude. Simulations were performed under constant pressure and temperature (NPT ensemble) using Langevin dynamics with a damping factor of 1 ps−1 and Nose-Hoover Langevin piston method with a damping time constant of 50 fs and decay period of 100 fs as described. Long-range electrostatic forces were simulated using the particle mesh Ewald summation with a grid size smaller than 1 Å. Full electrostatic interactions were calculated every 4th step. Van der Waals interactions were calculated using a switching function starting at 10 Å with a cutoff at 12 Å. Rigid bond lengths and angles of water molecules were used and an integration step of 1 fs was chosen.

All simulations were performed on a Cray XE6 at the Swiss National Supercomputing Centre.

Supplemental References

1. Schneider, C. A., Rasband, W. S. & Eliceiri, K. W. NIH Image to ImageJ: 25 years of image analysis. *Nat. Methods* **9**, 671-675 (2012).

2. Tse, J. R. & Engler, A. J. Preparation of hydrogel substrates with tunable mechanical properties. *Curr. Protoc. Cell. Biol.* **Chapter 10**, Unit 10.16 (2010).

3. Gao, M. *et al.* Structure and functional significance of mechanically unfolded fibronectin type III1 intermediates. *Proc. Natl. Acad. Sci. U. S. A.* **100**, 14784-14789 (2003).

4. Phillips, J. C. *et al.* Scalable molecular dynamics with NAMD. *J. Comput. Chem.* **26**, 1781-1802 (2005).

5. MacKerell,A.D. *et al.* All-Atom Empirical Potential for Molecular Modeling and Dynamics Studies of Proteinsâ€ . *J Phys Chem B* **102**, 3586-3616 (1998).

6. Krimm, I. *et al.* The Ig-like structure of the C-terminal domain of lamin A/C, mutated in muscular dystrophies, cardiomyopathy, and partial lipodystrophy. *Structure* **10**, 811-823 (2002).

7. Jorgensen, W. L., Chandrasekhar, J., Madura, J. D., Impey, R. W. & Klein, M. L. Comparison of simple potential functions for simulating liquid water. *J. Chem. Phys.* **79**, 926-935 (1983).

8. Humphrey, W., Dalke, A. & Schulten, K. VMD: visual molecular dynamics. *J. Mol. Graph.* **14**, 33-8, 27-8 (1996).

9. Swift, J. *et al.* Nuclear lamin-A scales with tissue stiffness and enhances matrix-directed differentiation. *Science* **341**, 1240104 (2013).

Supplemental Figures

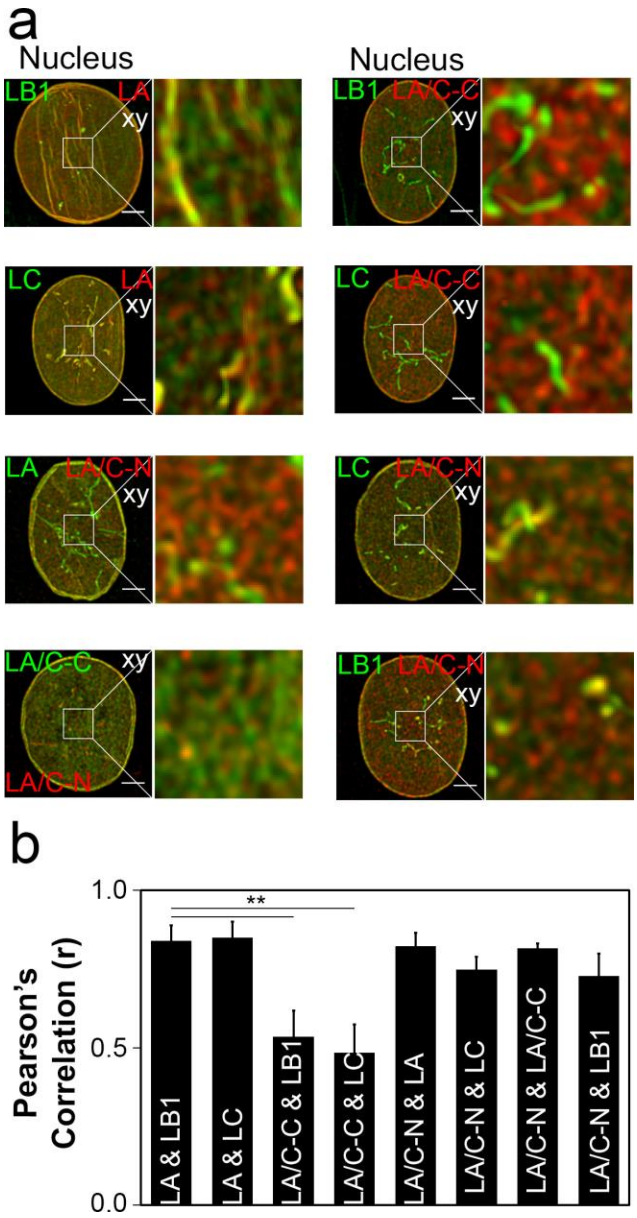

Figure S1. Pearson's correlation coefficient (r) is lower in nuclear immunostains of the LA/C-C antibody versus the LB1 or LC antibodies, but is high for all the other LA/C-N, LA, LC or LB1 antibody pairs.

a, Confocal z-axis maximum intensity projections of five representative nuclear lamin immunostains. The targeted proteins and corresponding antibodies are: lamin B1 (LB1), lamin A (LA), lamin C (LC), N-terminal lamin A/C (LA/C-N) and C-terminal lamin A/C (LA/C-C). Cells on Fn-coated glass were fixed 120 min after seeding. Scale bars: 3 µm. **b,** Spatial correlation between nuclear distributions of different lamin stains, based in the corresponding Pearsons' correlation coefficient between the intensities of different antibody pairs. **P<0.01

(Mann–Whitney U-test, two-tailed). Error bars represent the s.d. of the averages of 12 – 20 cells from 2 replicates.

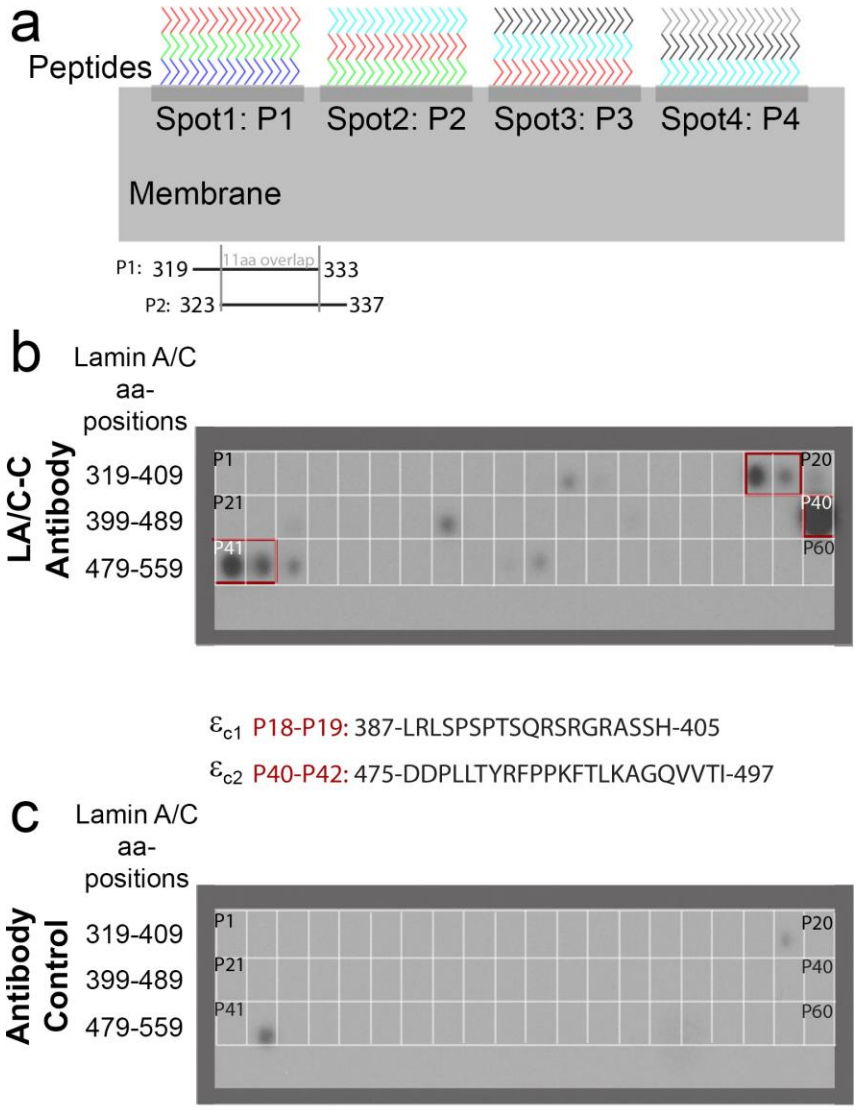

Figure S2. PepSpot™ based mapping and characterization of the epitope of the LA/C-C antibody indicating that it recognizes two separate regions (ε_{c1} and ε_{c2}) within the lamin A/C sequence

a, Schematic representation of the spotted peptides on the PepSpot™ membrane where 15 amino acid long peptides are immobilized. The peptide on one spot have an 11 amino acid sequence overlap with those on the next spot. **b,** The PepSpot™ membrane assay was performed with the LA/C-C antibody, whereby the peptide array covered the amino acids 319 to 566 of lamin A/C, the sequence which was specified by the supplier. Two distant peptide sequences are most strongly recognized by the antibody, spanning from P18-P19 (**ε_{c1}**) and P40-P42 (**ε_{c2}**) (red rectangles). The corresponding lamin A/C amino acid sequences forming the structural epitope (**ε_{c1}-ε_{c2}**) are given bellow. **c,** Antibody isotype control blot.

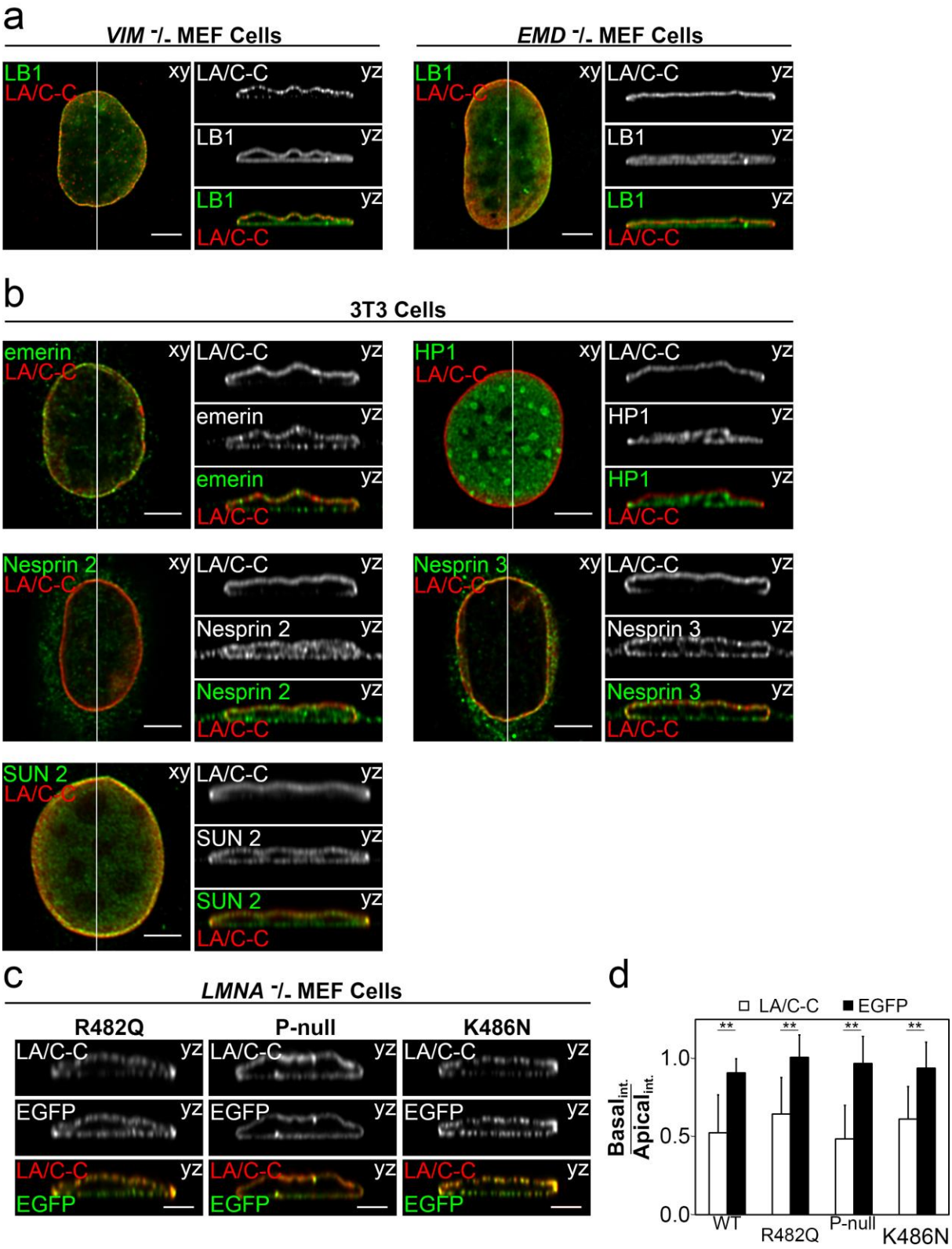

Figure S3. Vimentin null (*VIM* -/-), or emerin null (*EMD* -/-), or certain mutations in lamin A, do not interfere with the build-up of the LA/C-C basal-to-apical polarization in the NE. Furthermore, selected lamin A/C associated proteins do not show polarized distributions within the NE.

a, MEFs lacking either vimentin (VIM $^{-/-}$), an important intermediate filament, or emerin (EMD $^{-/-}$), a direct inner nuclear membrane binding partner of lamin A/C, were fixed 120 min after cell seeding on Fn-coated glass. xy- and yz-Confocal cross sections were obtained from the respective nuclei immunostained for LB1 (green) and LA/C-C (red). Scale bar 3µm. **b,** Different nuclear lamina associated proteins that are either part of the LINC complex (SUN 2), or bind to the LINC complex (Nesprin 3), or bind to the Ig-domain of lamin A/C (emerin, heterochromatin protein 1 (HP1) were immunostained and are shown together with LA/C-C antibody immunostainings in 3T3 cells on Fn-coated glass, 120 min after seeding. xy- and yz-confocal cross sections of nuclei immunostained for respective nuclear proteins (green) and LA/C-C (red). Scale bar 5µm. **c,** *LMNA* $^{-/-}$ MEF cells were rescued either with wt- or mutated lamin A. We selected mutations that affect DNA binding (R482Q), abolish the phosphorylation in the region 397 – 405 (P-null, S390A, S392A, S395A and S404A), or a residue required for sumoylation (K486N). Both single point mutations (R482Q and K486N) are associated with different laminopathies. yz-Confocal cross sections of *LMNA* $^{-/-}$ nuclei expressing different mutants, EGFP (green) and stained with LA/C-C (red). Scale bars 3 µm. **d,** Average basal-to-apical peak intensity ratios from the respective conditions. **P<0.01 (Mann–Whitney U-test, two-tailed). Error bars represent the s.d. of the averages of 21 – 24 cells from 2 replicates.

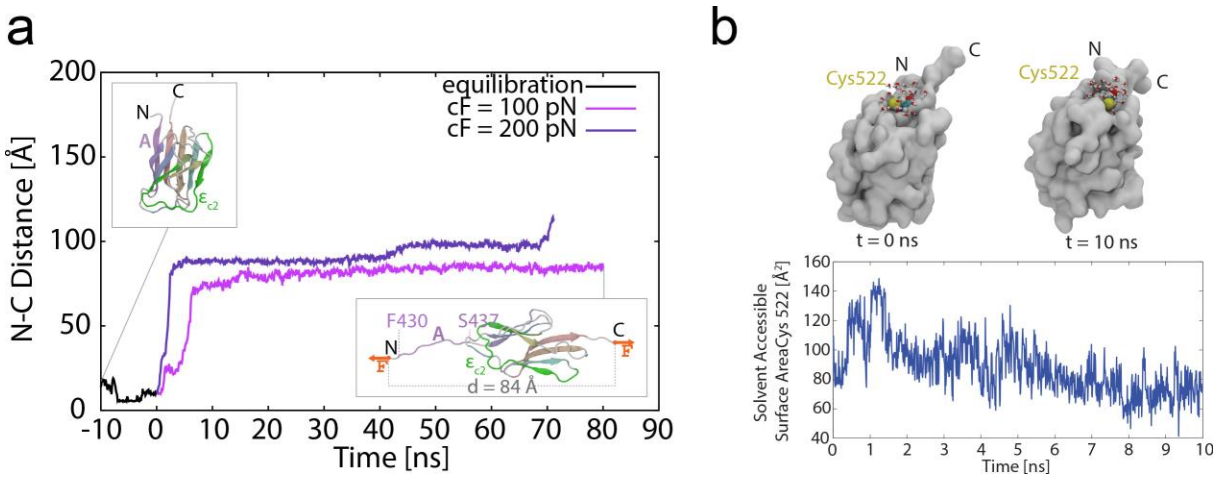

Figure S4. Steered molecular dynamics (SMD) simulations predict the existence of a well-pronounced structural intermediate state of the Ig-like domain of Lamin A upon stretching

a, For the SMD simulation of the Ig-like domain, its equilibrium structure[6] was immersed in a box filled with explicit water (see Supplemental Extended Experimental Procedures Section). After 10 ns of equilibration, constant force (cF) of either 100 or 200 pN was applied to the two terminal Cα atoms of S428 and V549 of the Ig-like domain in opposite direction but with equal magnitude. A stable structural intermediate is found in both simulations, for which the A-strand was pulled out of the Ig-fold, while the remaining Ig domain (β-strands B-H), which includes the scaffold that defines the ε_{c2}, remained unperturbed. This suggests a spatial separation of the ε_{c1}-linker-ε_{c2} epitope region. **b**, Molecular dynamic simulations further indicated that the Cys522, previously implicated to play a role in mechanoregulated processes[9], is already exposed to water in the equilibrated structure of the Ig-fold, as shown here by plotting the solvent accessible surface area of Cys522 during the 10 ns equilibration phase of the simulation shown in (a).

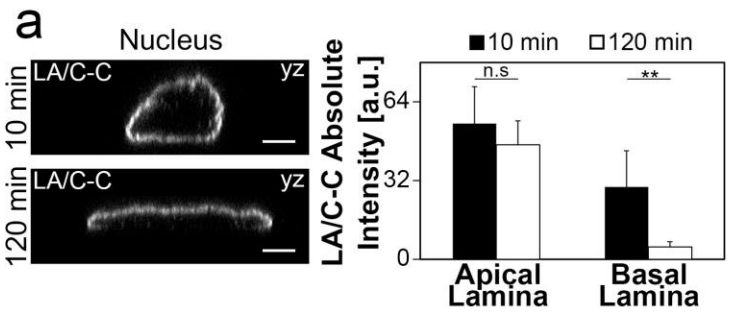

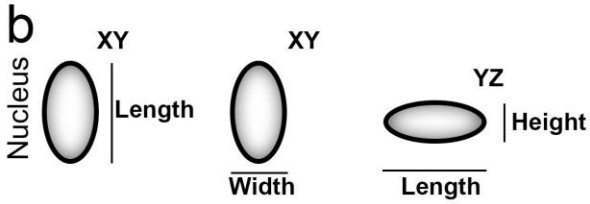

	XY Length [µm]	XY Width [µm]	Height [µm]
2 min	10.1 ± 1.2	7.9 ± 0.7	7.4 ± 0.8
10 min	12.3 ± 1.6	9.9 ± 1.6	6.1 ± 1.9
30 min	18.6 ± 2.4	14.2 ± 1.9	3.1 ± 1.3
60 min	21.0 ± 2.5	16.1 ± 2.3	2.6 ± 0.5
120 min	22.5 ± 2.4	15.9 ± 2.3	2.5 ± 0.5

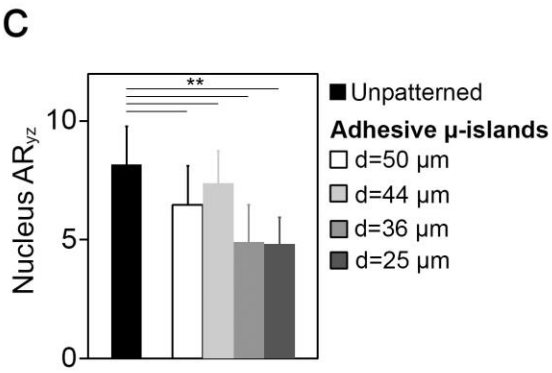

Figure S5. The LA/C-C antibody shows reduced binding to the basal side of the NE in spread 3T3 fibroblasts. The nuclear shape changes occur during cell spreading on Fn-coated glass and upon confinement on circular adhesive µ-islands of different diameters. **a,** Unprocessed yz-confocal cross sections of nuclei showing the LA/C-C intensity distributions along the NE (grey), 10 min (top) and 120 min (bottom) after cell seeding. All nuclei were imaged with the same PMT detector sensitivity. Scale bars: 3 µm. Average absolute LA/C-C basal and apical peak intensities. **P<0.01, n.s.= not significant (Mann–Whitney U-test, two-tailed). Error bars represent the s.d. of the averages of 7 and 10 cells. **b**, Nuclear length, width and height changes during cell spreading on Fn-coated glass (mean ± s.d.). Data represent the averages of 30 – 61 cells from 2 – 4 replicates. **c,** Average nuclear AR_{yz} as cells are confined

to adhesive micro-islands of different diameters (d), versus unpatterend Fn-coated glass, 4 h after seeding. Nuclear flattening was quantified by ellipse fitting to the nucleus yz-side profile. **P<0.01 (Mann–Whitney U-test, two-tailed). Error bars represent the s.d. of the averages of 30 – 55 cells from 3 – 4 replicates.

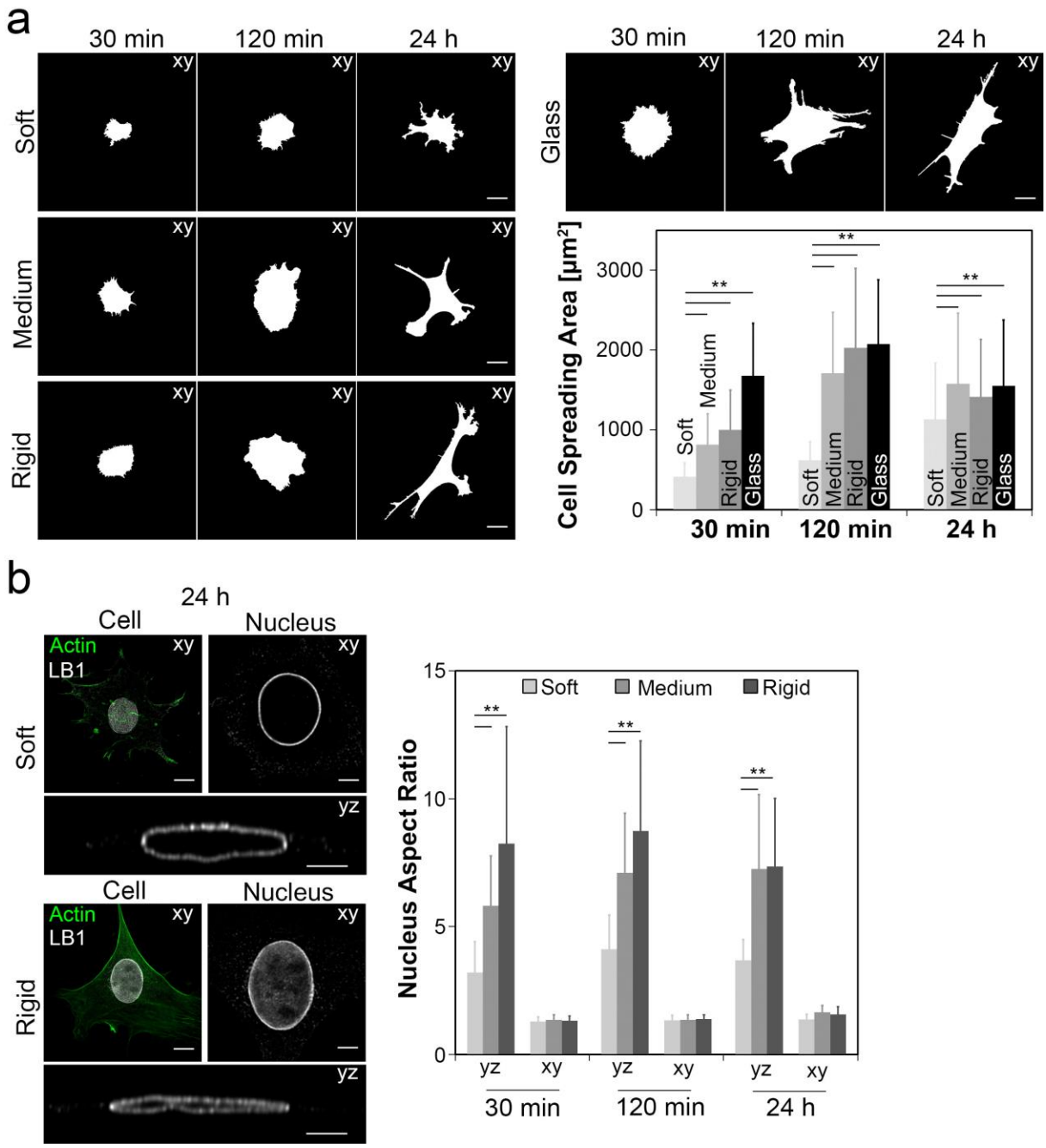

Figure S6. 3T3 fibroblasts spread more on rigid compared to soft Fn-coated polyacrylamide (PAA) gels and their nuclei become flatter

a, Binarized confocal images of representative cells on soft (0.4 kPa) medium (10 kPa) and rigid (30 kPa) Fn-coated PAA for the indicated time periods after seeding, as well as on Fn-coated glass. Average cell spreading areas for above mentioned conditions. **P<0.01 (Mann–Whitney U-test, two-tailed). Error bars represent the s.d. of the averages of 138 – 262 cells from 2 replicates. **b,** xy-Confocal cross sections of immunostained cells (actin, green; LB1, grey) spread on soft (top) and rigid (bottom) Fn-PAA together with corresponding nuclear xy- and yz-confocal cross sections. Average nuclear aspect ratios (AR_{xy} and AR_{yz}) measured over adhesion time and different PAA substrate rigidities. **P<0.01 (Mann–Whitney U-test, two-

tailed). Error bars represent the s.d. of the averages of 20 – 22 cells from 2 replicates. Scale bars: 20 µm for whole cell images and 5 µm for the nuclear images.

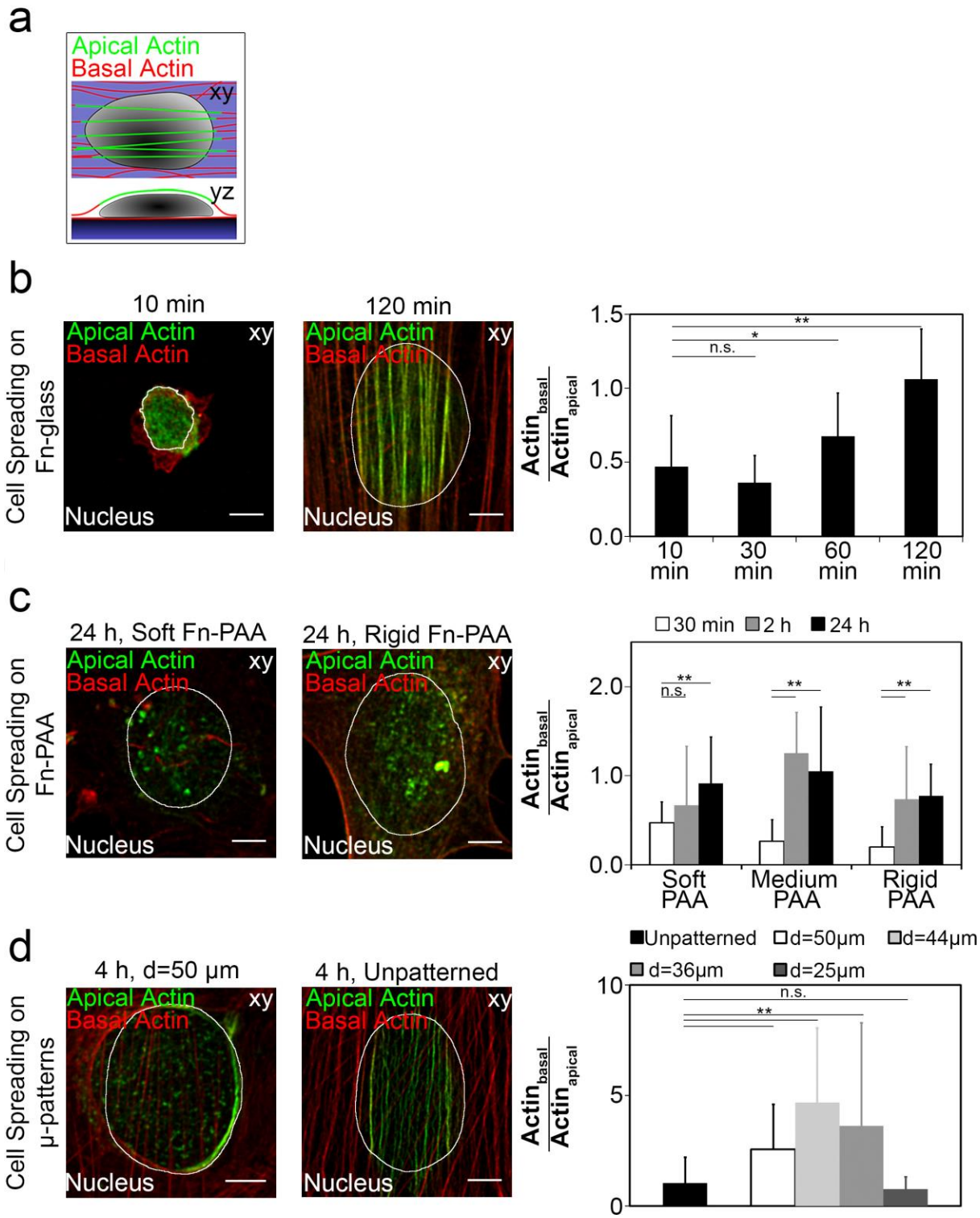

Figure S7. Basal-to-apical actin ratios change during 3T3 fibroblast spreading on either Fn-coated glass, on Fn-coated polyacrylamide gels with different rigidities, or if confined to different sized adhesive micro-islands

a, Schematic representation of the apical (green) and basal (red) actin distribution. **b, xy-**Confocal maximum intensity projection of phalloidin immunostain and average peak intensity ratios of f-actin accumulated below (basal, red) and above (apical, green) the nucleus after cell

seeding for indicated time periods on Fn-coated glass. **c,** Same analysis for cells seeded on Fn-coated PAA-substrates with different rigidities (previously defined in Fig. S6). **d,** Same analysis for cells confined to different sized circular adhesive μ-islands with diameter, d. *P<0.05, **P<0.01, n.s.= not significant (Mann–Whitney U-test, two-tailed). Error bars represent the s.d. of the averages of 10 – 32 cells from 2 – 3 replicates. Scale bars 5μm.

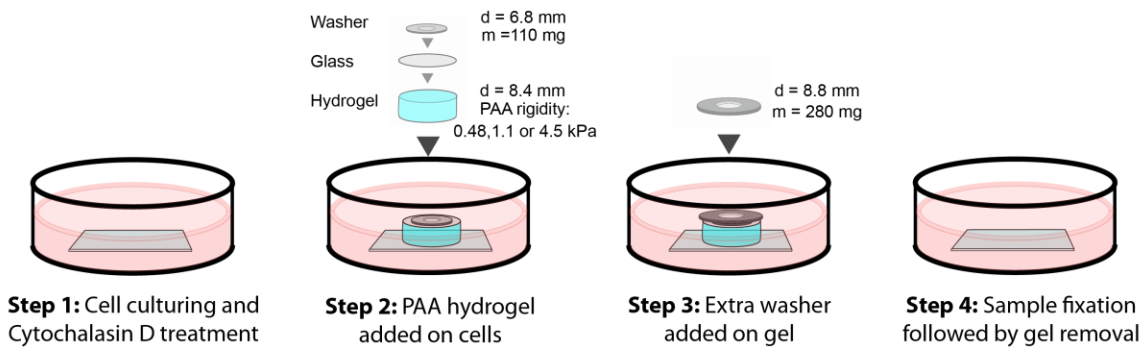

Figure S8. PAA-hydrogel cushions assay used to impose compressive pressure onto cells in 2-D cell culture.

Description of the different steps involving the respective components assembly in this experimental setup. **Step 1:** the cells are cultured on a Fn-coated glass coverslip, or alternatively, on a 0.48kPa Fn-coated PAA gel substrate (see Fig. 5h-k) for 24 h after seeding and afterwards are subjected to 5µg/ml Cytochalsin D (for 75 min or 60 min for cells seeded on Fn-PAA substrate). **Step 2:** The prefabricated PAA-cushion is carefully placed on top of the cells **Step 3:** Immediately after placing the PAA-cushion an extra weight is added to the gel in order to stabilize the PAA-cushion and apply extra pressure on cells (45min or 30min for cells seeded on Fn-PAA substrate) **Step 4:** While still under the PAA-cushion the cells are fixed by adding PFA (final concentration 2 %) directly to the cell culture medium (30 min). Afterwards, the PAA-cushion is carefully removed and the sample is immunolabeled. (see Supplementary Materials and Methods and Fig. 5d-k)